HHS Public Access

Author manuscript

J Cell Physiol. Author manuscript; available in PMC 2024 November 01.

Published in final edited form as:

J Cell Physiol. 2023 November ; 238(11): 2668–2678. doi:10.1002/jcp.31120.

Loss of *miR-204* and *miR-211* shifts osteochondral balance and causes temporomandibular joint osteoarthritis

Jian Huang[1], **Yumei Lai**[1], **Jun Li**[1], **Lan Zhao**[1]

[1]Department of Orthopedic Surgery, Rush University Medical Center, Chicago, IL 60612, USA.

Abstract

Temporomandibular joint (TMJ) osteoarthritis (OA) is a common type of TMJ disorders causing pain and dysfunction in the jaw and surrounding tissues. The causes for TMJ OA are unknown and the underlying mechanism remains to be identified. In this study, we generated genetically-modified mice deficient of two homologous microRNAs, *miR-204* and *miR-211*, both of which were confirmed by in situ hybridization to be expressed in multiple TMJ tissues, including condylar cartilage, articular eminence, and TMJ disc. Importantly, the loss-of-function of *miR-204* and *miR-211* caused an age-dependent progressive OA-like phenotype, including cartilage degradation and abnormal subchondral bone remodeling. Mechanistically, the TMJ joint deficient of the two microRNAs demonstrated a significant accumulation of RUNX2, a protein directly targeted by *miR-204/−211*, and upregulations of β-catenin, suggesting a disrupted balance between osteogenesis and chondrogenesis in the TMJ, which may underlie TMJ OA. Moreover, the TMJ with *miR-204/−211* loss-of-function displayed an aberrant alteration in both collagen component and cartilage-degrading enzymes and exhibited exacerbated orofacial allodynia, corroborating the degenerative and painful nature of TMJ OA. Together, our results establish a key role of *miR-204/−211* in maintaining the osteochondral homeostasis of the TMJ and counteracting OA pathogenesis through repressing the pro-osteogenic factors including RUNX2 and β-catenin.

Keywords

Osteoarthritis; Temporomandibular joint; Orofacial pain; MicroRNA; RUNX2; NGF; β-catenin

Introduction

The temporomandibular joint (TMJ) is a unique synovial articulation that connects the mandible to the temporal bones of the skull. It has a complex structure including the mandibular condyle, articular disc, and articular eminence/glenoid fossa, of which the integrity is essential to three-direction motion of the jaw. TMJ disorders (TMD) cause

Correspondence: Lan Zhao, Department of Orthopedic Surgery, Rush University Medical Center, Chicago, IL 60612, USA. lan_zhao@rush.edu.

Author contributions

J.H. designed the research, performed experiments, analyzed data, and wrote the manuscript. Y.L. performed experiments and analyzed data. J.L. performed mouse von Frey tests. L.Z. designed the project, performed experiments, analyzed the results, and revised the manuscript.

Conflict of Interest Statement

The authors declared no potential conflicts of interest with respect to the research, authorship, and/or publication of this article.

pain and dysfunction in the jaw and surrounding tissues, therefore the patients of TMD have difficulties in chewing, swallowing, speaking and making facial expressions (Matheus, Özdemir Ş, & Guastaldi, 2022; Nickel, Iwasaki, Gonzalez, Gallo, & Yao, 2018). It is estimated that as high as 30% of the adult population are affected by TMD (Valesan et al., 2021) and that over 10 million U.S. adults developed clinically verified TMD annually (Slade et al., 2016). One important subtype of TMD is TMJ osteoarthritis (OA), which is characterized by progressive cartilage degradation and aberrant subchondral bone remodeling. The causes of most TMD, including TMJ OA are unknown and the underlying mechanism remains to be identified.

Recent progresses in TMJ OA research have gained insights from genetic mouse models, which involve multiple signaling pathways (Hill, Duran, & Purcell, 2014; Koyama et al., 2014; Liao et al., 2019; Lu et al., 2022; Mori, Izawa, & Tanaka, 2015; M. Wang et al., 2014). Our previous results demonstrate that activation of the Wnt/β-catenin signaling in condylar chondrocytes leads to degenerative defects resembling TMJ OA (Hui et al., 2018; Zhou et al., 2019). Smad3 deficiency results in erosion of the articular cartilage of the mandibular condyles (Mori et al., 2015). *Prg4*$^{-/-}$ mice show OA-like lesions including synovial hyperplasia, deterioration of cartilage in the condyle, disc and fossa, suggesting the importance of lubricin in the maintenance of TMJ (Hill et al., 2014; Koyama et al., 2014). These findings in TMJ OA parallel those in knee joint OA, pointing to a similarity between TMJ OA and knee joint OA in pathogenic mechanism. Importantly, a variety of knee joint OA mouse models, including genetic mouse models and surgically-induced OA models (Chen, Thuillier, Chin, & Alliston, 2012; Kawaguchi, 2008; Shen et al., 2013), displayed an up-regulation of Runx2 in OA pathogenesis, along with a TMJ OA model, namely *Ddr1* knockout mice (Schminke et al., 2014). Since Runx2 is a key transcription factor directly regulating the expression of matrix degradation enzymes, such as MMP13 and ADAMTS5, Runx2 up-regulation in OA pathogenesis could underlie the mechanism of cartilage degradation, the pivotal phenotype observed in both TMJ OA and knee joint OA.

We have identified two homologous miRNAs, *miR-204* and *miR-211*, which negatively regulate Runx2 in skeletal progenitor cells (Huang, Zhao, Xing, & Chen, 2010). To further study the *in vivo* functional roles of *miR-204/−211*, we have generated *miR-204* and *miR-211* double knockout (dKO) mice, which exhibits a spectrum of pathological changes, mostly aging-related, such as hypermature cataracts with rupture, uveal melanosis, and retinal dysplasia in eyes, follicular dysplasia in skins, valvular endocardiosis in hearts, and OA in knee joints (Huang et al., 2019). In this study, we examined the in situ expression of *miR-204* and *miR-211* in the TMJ, and investigated whether the loss-of-function of the miRNAs affected TMJ joint pathophysiology. Interestingly, we found that the dKO mice developed spontaneous TMJ OA-like phenotype, including cartilage degradation, abnormal remodeling of condylar subchondral bone, and orofacial allodynia. In condylar cartilage, Runx2 was significantly induced by the deletions of *miR-204/−211*, which resulted in abnormal production of cartilage-catabolic enzymes and matrix components. Moreover, our immunohistochemistry data revealed an upregulation of β-catenin in the TMJ tissues that may underlie cartilage degeneration and subchondral sclerosis. In summary, our results demonstrate that *miR-204/−211* are key regulators in maintaining TMJ homeostasis

and counteracting OA pathogenesis by regulating Runx2 and β-catenin, both important transcriptional factors controlling OA pathogenesis.

Materials and Methods

Animals

The *miR-204* and *miR-211* floxed mice were generated as described previously (Huang et al., 2019). *CMV-Cre* mice (The Jackson Laboratory, Bar Harbor, ME, USA) were crossed with *miRNA* floxed mice to generate germline deletions of the *miRNAs* (*miR-204*$^{flox/flox}$; *miR-211*$^{flox/flox}$; *CMV-Cre*). All the experimental procedures were approved by the Institutional Animal Care and Use Committee of Rush University Medical Center.

Micro-CT, histology and histomorphometry

For μCT scanning, we used a Scanco μCT35 scanner (Scanco Medical, Brüttisellen, Switzerland) with 70 kVp source and 114 μA current for formalin-fixed mouse heads with a resolution of 10 μm. For histology, tissues were fixed in 10% formalin, decalcified, and embedded in paraffin. Serial sagittal sections of TMJs were cut every 3 μm. The sections were stained with Alcian blue/hematoxylin & orange G (AB/H&OG) for histological analysis as previously described (Fan, Zhao, Lai, Lu, & Huang, 2022; L. Zhao et al., 2019). OARSI scoring was performed to evaluate condylar cartilage destruction essentially as previously described (Glasson, Chambers, Van Den Berg, & Little, 2010). Specifically, condylar cartilage areas of the stained tissue sections were scored by a recommended 0–6 subjective scoring system. Histomorphometric measurements, like cartilage area and thickness, were performed using OsteoMeasure software (OsteoMetrics, Inc., Atlanta, GA, USA). Specifically, condylar cartilage area was measured based on positive staining of Alcian blue. For the calculation of average condylar cartilage thickness, three lines indicating the thickness from the middle area of the stained cartilage were drawn and measured. The numbers were averaged for an average cartilage thickness.

In situ hybridization (ISH) and immunohistochemistry (IHC)

We performed ISH on 3-μm-thick sections using the microRNA ISH Buffer and Controls Kit (Exiqon, Vedbaek, Denmark) as previously described. Briefly, sections were treated with Proteinase K for 15 minutes at room temperature, 3% H_2O_2 for 10 minutes to block endogenous peroxidase activity and then dehydrated before applying 40 nM double-DIG LNA™ microRNA probe for *miR-204* or *miR-211*, both of which were purchased from Exiqon. Hybridization was performed for 1 hour at 53°C for *mmu-miR-204*, and 48°C for *mmu-miR-211* respectively. Anti-DIG-POD antibody (Roche Applied Science, Indianapolis, IN, USA) and TSA-plus FITC substrate (Perkin Elmer, Waltham, MA, USA) were applied for detection of fluorescent signal. VECTASHIELD Mounting Medium with DAPI (Vector Laboratories, Burlingame, CA, USA) was used to mount the slides. IHC was performed as previously described (Fan et al., 2022). Briefly, 3 μm paraffin sections were heated at 95°C for 10 minutes or 75°C for 30 minutes in Antigen Unmasking Solution (Vector Laboratories, Burlingame, CA, USA), and then sequentially treated with 3% H_2O_2, 0.5% Triton X-100, Avidin/Biotin Blocking Kit (Invitrogen, Carlsbad, CA, USA). After blocking with 10% normal goat serum (Vector Laboratories, Burlingame, CA, USA) for 1 hour, sections

were treated with 1/200 anti-Runx2 antibody (D130–3, MBL, Woburn, MA, USA), 1/200 MMP13 antibody (ab39012, Abcam, Cambridge, MA, USA), 1/500 Adamts5 antibody (ab41037, Abcam, Cambridge, MA, USA) and 1/500 Lubricin antibody (ab28484, Abcam, Cambridge, MA, USA) overnight at 4°C and incubated with 1/400 secondary biotinylated goat anti-rabbit or anti-mouse antibody (Vector Laboratories, Burlingame, CA, USA) for 30 minutes, followed by treatment with VECTASTAIN Elite ABC Kit (Vector Laboratories, Burlingame, CA, USA). IHC signals were revealed by ImmPACT DAB Peroxidase Substrate (Vector Laboratories, Burlingame, CA, USA). For fluorescent IHC, sections were incubated with 1/200 Type II collagen antibody (ab3092, Abcam, Cambridge, MA, USA), 1/1000 Type X collagen antibody (234196, EMD Millipore, Billerica, MA, USA), 1/100 β-catenin Antibody (610154, BD Biosciences), 1/200 β-III Tubulin Antibody (R&D Systems, Minneapolis, MN, USA) and 1/200 NGF antibody (ab6199, Abcam, Cambridge, MA, USA) overnight at 4°C and then incubated with secondary antibody conjugated to Alexa Fluor 488 or 594 (Invitrogen, Carlsbad, CA, USA) for 30 minutes. Images of histology, ISH and IHC were captured using CellSens Imaging Software (Olympus) on an Olympus BX43 microscope, or a Zeiss LSM700 confocal microscope. Positive signals of IHC were quantified using ImageJ.

Quantitative reverse-transcription PCR (qRT-PCR)

For profiling gene expressions, total RNA was extracted from the condylar cartilage and qRT-PCR was performed, using the primer pairs for *Runx2* (5’-CAAGAAGGCTCTGGCGTTTA-3’ and 5’-TGCAGCCTTAAATGACTCGG-3’), *Mmp13* (5’-CTTCTTCTTGTTGAGCTGGACTC-3’ and 5’-CTGTGGAGGTCACTGTA GACT-3’), *Adamts5* (5’-GGAGCGAGGCCATTTACAAC-3’ and 5’-CGTAGACAAGGTAG CCCACTTT-3’), *Aggrecan* (5’-CCTGCTACTTCATCGACCCC-3’ and 5’-AGATGCTGTTGACTCGAACCT-3’), *Col2a1* (5’-GGGAATGTCCTCTGCGATGAC-3’ and 5’-GAAGGGGATCTCGGGGTTG-3’), *Col10a1* (5’-TTCTGCTGCTAATGTTCTTGACC-3’ and 5’-GGGATGAAGTATTGTGTCTTGGG-3’), and *β-actin* (5’-GGCTGTATTCCCCTCCATCG-3’ and 5’-CCAGTTGGTAACAATGCCATGT-3’). Specifically, for mouse *miR-204* and *miR-211* qRT-PCR, the reverse transcription primer is *mmu-miR-204/−211-RT* (5’-GTCGTATCCAGTGCAGGGTCCGAGG TATTCGCACTGGATACGACAGGCAW-3’), and the quantitative PCR primers are *mmu-miR-204* forward (5’-GGGCTTCCCTTTGTCATCCTAT-3’), *mmu-miR-211* forward (5’-GGGCTTCCCTTT GTCATCCTT-3’) and the reverse primer (5’-CCAGTGCAGGGTCCGAGGT-3’).

Animal behavior tests

Testing for orofacial mechanical allodynia (von Frey sensitivity) was performed essentially according to a method previously described (Chaplan, Bach, Pogrel, Chung, & Yaksh, 1994). Before the von Frey test, we allowed animals to adapt to the environment for 15 minutes. A calibrated set of von Frey filaments (Stoelting, Wood Dale, IL) was used to poke the skin around TMJ to calculate the head withdrawal threshold. Briefly, ascending series of the filaments were used. Each filament was applied five times at an interval of a few seconds. The response threshold was defined as the lowest force of the filaments causing head withdrawal observed at least three times out of five tests. The tests were performed in a

blind manner that the investigator is not aware of the identification of animals as well as the study groups. The grooming activities were measured using Laboratory Animal Behaviour Observation, Registration and Analysis System (LABORAS), according the manufacturer's instruction.

Statistical analyses

All the data were expressed as mean ± s.d, as indicated in the figure legends. Statistical analyses were completed with Prism GraphPad. Unpaired Student's *t*-test or Mann-Whitney test was performed and indicated in the figure legends. $P < 0.05$ was considered statistically significant.

Results

Deficiency of *miR-204* and *miR-211* induces TMJ OA.

To determine the expression of *miR-204* and *miR-211* in the mouse TMJ, we performed in situ hybridization (ISH) assay using highly specific locked nucleic acid (LNA)-enhanced miRNA probes. Our findings demonstrated that both *miR-204* and *miR-211* are expressed in the TMJ tissues, including condylar cartilage, articular eminence, and TMJ disc (Figure 1A, B). We also generated the deletions of *miR-204* and *miR-211* in germlines by crossing the *miR-204*$^{flox/flox}$ and *miR-211*$^{flox/flox}$ mice with *CMV-Cre* transgenic mice and breeding the progeny with C57BL6/J for generations to remove *CMV-Cre*. The resultant constitutive dKO mice can serve as a negative control for the ISH experiment. Our results demonstrated complete loss of *miR-204* (Figure 1C) or *miR-211* (Figure 1D) in the TMJ tissues, suggesting that both *miRNAs* have been effectively deleted. In addition, reverse transcription quantitative PCR (RT-qPCR) results also demonstrated significant decrease of *miR-204* (Figure 1E) and *miR-211* (Figure 1F) in condylar cartilage isolated from the dKO mice, compared with that in control (C57BL6/J) mice. Together, our results demonstrated that *miR-204* and *miR-211* are endogenous players in the TMJ and confirmed effective deletions of both miRNAs in the dKO mice.

To study the in vivo function of *miR-204* and *miR-211* in the TMJ, we analyzed the TMJ phenotype of the dKO mice by histology and μCT analyses. Firstly, we analyzed the 3-month-old dKO mice to investigate whether the dKO TMJs show a significant phenotype at young ages, which may indicate potential developmental effects of the miRNA deficiency. Both histology and μCT results didn't exhibit significant distinguishable changes in the dKO TMJ compared with the control tissues, as there were no significant differences in condylar cartilage thickness (Figure 2A) and subchondral bone mass and density (Figure 2B–G) between the control and dKO TMJs. Thus, our data suggested that the deficiency of *miR-204* and *miR-211* did not induce apparent defects in TMJ development and homeostasis when the mice are young.

Next, we focused on studying the TMJ in the 8-month-old dKO mice to study if the mice develop a TMJ phenotype with aging. The histology results showed significant proteoglycan loss and cartilage reduction (Figure 3A), as displayed by striking reductions of both intensity and thickness of alcian blue staining, suggesting an aging-dependent pathogenesis of TMJ

OA. Histomorphometric quantification of the condylar cartilage area and cartilage thickness confirmed significant degeneration of condylar cartilage in the dKO TMJ (Figure 3B, C). The Osteoarthritis Research Society International (OARSI) scoring also demonstrated severe destruction of condylar cartilage in the TMJ deficient of the two miRNAs (Figure 3D). To investigate if abnormal bone remodeling occurred in the dKO TMJ, we performed μCT scanning of the TMJ specimens and found that the dKO TMJ underwent abnormal remodeling in condylar subchondral bone. Specifically, the condylar subchondral bone in the dKO mice showed higher bone volume fraction (Figure 3E, F), greater bone mineral density (Figure 3G), and increased trabecular thickness (Figure 3I), with reduced trabecular separation (Figure 3J) and unchanged trabecular numbers (Figure 3H). Collectively, the *miR-204* and *miR-211* dKO mice developed severe TMJ OA, suggesting that *miR-204* and *miR-211* may play important roles in TMJ homeostasis that may protect joints against OA pathogenesis.

The *miR-204/−211*-RUNX2 axis is essential for joint homeostasis

We previously reported that *miR-204/−211* suppress Runx2 expression in skeletal progenitor cells. By performing immunohistochemistry (IHC) on the TMJ sections, we found that RUNX2 proteins accumulated in the TMJ tissues of the dKO mice (Figure 4A), particularly in condylar cartilage. This result suggested that ablation of *miR-204/−211* upregulates the protein level of RUNX2 in chondrocytes, which may induce TMJ OA pathogenesis. Moreover, MMP13 and ADAMTS5, two matrix proteases reported to be induced by RUNX2 and serve as representative OA markers, increased significantly in the dKO TMJ (Figure 4B, C). Quantification of IHC further demonstrated the significant upregulations of RUNX2, MMP13 and ADAMTS5 by the loss-of-function of *miR-204* and *miR-211* (Figure 4A–C). Moreover, the mRNA expression levels of *Runx2*, *Mmp13* and *Adamts5* in condylar cartilage of the dKO mice were also elevated significantly compared with those in the control mice (Figure 4E–G), while the mRNA expression level of *Aggrecan* in condylar cartilage of the dKO mice was decreased significantly (Figure 4H). On the other hand, the protein levels of lubricin, which is essential and major product in the synovial fluid and acts as a joint lubricant (Hill et al., 2014), decreased dramatically in the dKO condylar chondrocytes as shown by our IHC data and quantification (Figure 4D). Thus, our results suggest that the deficiency of *miR-204* and *miR-211* in TMJ upregulates RUNX2, which induces the expression of cartilage-degrading enzymes such as MMP13 and ADAMTS5 and reduces the expression of lubricin, a key factor maintaining joint integrity, both contributing to a profound pathogenesis of TMJ OA.

Collagens are main components in cartilage and their healthy turnover is essential for the integrity of articular cartilage. Degeneration and damage of cartilage during OA is associated with loss of type II collagen (Col2a1) and upregulation of type X collagen (Col10a1) (Bernabei, So, Busso, & Nasi, 2023; van der Kraan & van den Berg, 2012). As RUNX2 controls the differentiation of articular chondrocytes into hypertrophic chondrocytes that produce high levels of Col10a1, we performed fluorescent immunohistochemistry (IHC) to determine if RUNX2 accumulation in the chondrocytes of dKO TMJ resulted in degenerative changes of collagen production. Our results demonstrated that Col10a1 increased robustly in the dKO condylar cartilage, while Col2a1 decreased significantly

(Figure 5A, C). Quantification of the IHC results also confirmed a significant shift of collagen components from type II to type X in the dKO condylar cartilage, while the control samples retained higher amounts of type II collagen (Figure 5B, D). Moreover, the condylar cartilage of the dKO mice showed a significant decrease in *Col2a1* mRNA expression and a substantial increase in *Col10a1* expression compared to that of the control mice (Figure 5E, F). Since the cartilage expressing *Col10a1* initiates calcification in osteoarthritic joints, these results also suggested that deficiency of *miR-204* and *miR-211* induces pathological mineralization and degeneration of condylar cartilage in the dKO TMJ, which could be contributed by RUNX2, a major transcriptional regulator of chondrocyte hypertrophy and osteoblast differentiation.

Dysregulation of β-catenin signaling by *miR-204/−211* loss-of-function

It has been reported that the upregulation of the Wnt/β-catenin signaling pathway leads to the onset and progression of TMJ OA (Hui et al., 2018; M. Wang et al., 2014). Since both RUNX2 and β-catenin are master transcriptional factors governing bone formation and OA pathogenesis, we are interested to examine if the β-catenin level was enhanced as well in the dKO TMJ. Our IHC results confirmed that β-catenin was significantly increased in the TMJ void of the expressions of *miR-204* and *miR-211* (Figure 6A–C), mostly evident in the condylar cartilage. Interestingly, positive immunostaining of β-catenin (Figure 6B) was largely overlapping with those of RUNX2, cartilage-degrading enzymes (Figure 4), and Col10a1 (Figure 5), suggesting that β-catenin and RUNX2 may work in a synergy to induce catabolic and degenerative reactions in the condylar cartilage. Together, our results suggested that the miRNAs negatively regulate the β-catenin signaling, in addition to their repression of RUNX2, which both promote a degenerative response in the TMJ and eventually result in TMJ OA.

Insufficiency of *miR-204/−211* sensitizes TMJ OA pain

TMJ OA could be painful and it affects function of jaw and surrounding tissues. Thus, we performed behavioral tests to determine if the pain-related behavior was altered in the dKO mice. Our analysis using the Laboratory Animal Behaviour Observation, Registration and Analysis System (LABORAS) revealed that the dKO mice had significantly increased grooming behavior compared with the control group (Figure 7A), suggesting that the dKO mice might experience discomfort in their orofacial area. Further evaluation of orofacial allodynia by von Frey behavioral test showed significantly increased pain sensitivity related to the TMJ in the dKO mice compared with the control group (Figure 7B). Thus, our results strongly suggested that the *miR-204/−211* deficient mice have TMJ pain, which is associated with and could be induced by the TMJ OA phenotype in the dKO mice. To further investigate the change of neurological activities in the dKO TMJ, we performed IHC of neural factors including β-III tubulin, a neuronal marker required for axon guidance and maintenance, and nerve growth factor (NGF), a major growth factor of nociceptive pain (Seidel, Wise, & Lane, 2013). Our data demonstrated that both neural factors were significantly increased in the dKO TMJ (Figure 7C, D), therefore suggesting augmented neurite growth in dKO TMJ and excessive pain sensitivity in the dKO TMJ (Figure 7E, F). Collectively, our data suggested that *miR-204/−211* deficiency in the TMJ promotes OA pathogenesis and enhances orofacial pain.

Discussion

In this work, we used a new genetically-modified mouse model, in which *miR-204* and *miR-211* were deleted, to investigate the function of the two miRNAs in the TMJ. Our data demonstrated that loss-of-function of *miR-204/−211* significantly upregulated multiple pivotal skeletal factors including RUNX2 and β-catenin in the TMJ, which leads to induction of matrix-degrading enzymes and pain-associated factors, as well as aberrant changes in collagen components and lubricin. Thus, we have observed a comprehensive TMJ OA phenotype, which includes condylar cartilage degeneration, condylar subchondral bone sclerosis, and sensitization of TMJ OA pain. It is notable that the degenerative processes of the TMJ is often initiated by injury or overloading, which induces an inflammatory environment within the joint. As the deficiency of *miR-204* and *miR-211* upregulates RUNX2 and β-catenin, both of which promote chondrocyte hypertrophy and osteoblast differentiation (Catheline et al., 2019; Day, Guo, Garrett-Beal, & Yang, 2005; Hui et al., 2018), the dKO condylar chondrocytes failed to preserve a balance between healthy homeostasis and chondrocyte hypertrophy/osteogenic differentiation. Nevertheless, the dKO joint cells may also undergo dysregulation of additional signaling pathways, such as enhanced inflammatory reactions, since the inductions of catabolic enzymes and pain-related neural factors are also associated with inflammation, which could contribute to the onset and deterioration of the TMJ degeneration as well. Therefore, it would gain valuable insights to further explore if *miR-204* and *miR-211* play a significant role in modulating the responses of joint cells to inflammation, especially in the context of OA.

There are considerable similarities in terms of structural changes between knee joint OA and TMJ OA, as they both demonstrate whole-joint degeneration including articular cartilage degradation, abnormal subchondral bone remodeling, and generally chronic and low-grade synovial inflammation (Huang, Zhao, & Chen, 2018; X. D. Wang, Zhang, Gan, & Zhou, 2015). However, TMJ also retains distinct pathological features from those weight-bearing joints during OA conditions, because of its unique biochemical compositions in cartilage that is composed of both type I and type II collagen (Lu et al., 2022), as well as its complicated, three-dimensional movements. In our dKO mice, the miRNA deficiency altered the collagen composition of the condylar cartilage by reducing type II collagen, which is expected to have negative effects on the loading-bearing capacity of the condylar cartilage and thus accelerates its degeneration. Regarding subchondral bone degeneration, knee joint OA predominantly exhibit sclerosis, whereas TMJ OA frequently shows bone erosion. In this study, we found that the TMJ in the dKO mice had increased bone formation, which is different from subchondral bone loss observed from several TMJ OA models (Embree et al., 2011; Zhang et al., 2013). It is notable that our study was focused on aged mice that could reflect the late and relatively stable stages of TMJ OA, thus showing different pathology from the TMJ OA models at earlier stages. In addition, it has been demonstrated in the TMJ OA models that subchondral bone formation is increased in later stages after induction of resorptive activity in the initial phases (Zhang et al., 2013). In patients, sclerosis is frequently observed and thought to be indicative of later stages of the disease, compared to resorption (Alzahrani, Yadav, Gandhi, Lurie, & Tadinada, 2020; Koç, 2020; Nah, 2012; Y. P. Zhao, Zhang, Wu, Zhang, & Ma, 2011). Together, our observations from the dKO mice

may provide insights into cartilage degeneration and subchondral bone remodeling during TMJ OA.

The miRNAs are important players in the genetic network, which can provide genetic buffering and thus maintain the robustness of a biological system (Vidigal & Ventura, 2015). An average miRNA is estimated to bind to the 3'-UTR of their target genes that are numbered in hundreds and may include an army of master regulators of different pathways. Through regulating protein translation or mRNA stability, the miRNAs maintain the homeostasis of tissues and organs. The dKO mice did not show apparent gross abnormality at their young ages, for which the reason may be that the deficiency of *miR-204* and *miR-211* could be complemented by fluctuations of other factors in the same or related regulatory network. However, the TMJ OA phenotype became evident when the mice were 8 months old, which demonstrates that the deficiency of the miRNAs have cumulative effects in dysregulating the TMJ pathophysiology. While our study used a constitutive KO model, our data suggested that the phenotype should result from the deficiency of the miRNAs in skeletal progenitor cells and their decedents that include chondrocytes, osteoblasts, and fibroblast-like synoviocytes, since the miRNAs have extensive expression in multiple type of TMJ cells and their loss-of-function leads to a comprehensive whole-joint phenotype. Moreover, the germline deletions of the *miRNAs* may induce pathological changes in extensively additional types of tissues and cells that are not limited to joint cells, including those of the immune and nerve systems. For example, the altered pain behavior could be collectively attributed to structural changes in the TMJ as well as the dysregulation of inflammatory and neuronal activities in the dKO mice. Thus, our study has its limitation as it could not exclude whether the deficiency of *miR-204* and *miR-211* dysregulates non-skeletal cell types during TMJ OA, which is interesting and warrants future investigations of the dKO mice, a unique mouse model of aging. Together, our results establish an essential role of *miR-204* and *miR-211* in maintaining osteochondral homeostasis that protects the joint against OA, and demonstrate a translational potential of using the miRNAs as therapeutic agents to treat TMJ OA.

Acknowledgments

The authors disclosed receipt of the following financial support for the research, authorship, and/or publication of this article: J. Huang and L. Zhao were supported by the National Institute of Arthritis and Musculoskeletal and Skin Diseases of National Institutes of Health (R01AR070222, and R01AR070222-04S1).

Data Availability Statement

The data that support the findings of this study are available within the article or from the corresponding author upon reasonable request.

References

Alzahrani A, Yadav S, Gandhi V, Lurie AG, & Tadinada A (2020). Incidental findings of temporomandibular joint osteoarthritis and its variability based on age and sex. Imaging Sci Dent, 50(3), 245–253. doi: 10.5624/isd.2020.50.3.245 [PubMed: 33005582]

Bernabei I, So A, Busso N, & Nasi S (2023). Cartilage calcification in osteoarthritis: mechanisms and clinical relevance. Nat Rev Rheumatol, 19(1), 10–27. doi: 10.1038/s41584-022-00875-4 [PubMed: 36509917]

Catheline SE, Hoak D, Chang M, Ketz JP, Hilton MJ, Zuscik MJ, & Jonason JH (2019). Chondrocyte-Specific RUNX2 Overexpression Accelerates Post-traumatic Osteoarthritis Progression in Adult Mice. J Bone Miner Res, 34(9), 1676–1689. doi: 10.1002/jbmr.3737 [PubMed: 31189030]

Chaplan SR, Bach FW, Pogrel JW, Chung JM, & Yaksh TL (1994). Quantitative assessment of tactile allodynia in the rat paw. J Neurosci Methods, 53(1), 55–63. doi: 0165–0270(94)90144–9 [pii] [PubMed: 7990513]

Chen CG, Thuillier D, Chin EN, & Alliston T (2012). Chondrocyte-intrinsic Smad3 represses Runx2-inducible matrix metalloproteinase 13 expression to maintain articular cartilage and prevent osteoarthritis. Arthritis Rheum, 64(10), 3278–3289. doi: 10.1002/art.34566 [PubMed: 22674505]

Day TF, Guo X, Garrett-Beal L, & Yang Y (2005). Wnt/beta-catenin signaling in mesenchymal progenitors controls osteoblast and chondrocyte differentiation during vertebrate skeletogenesis. Dev Cell, 8(5), 739–750. doi: 10.1016/j.devcel.2005.03.016 [PubMed: 15866164]

Embree M, Ono M, Kilts T, Walker D, Langguth J, Mao J, … Young M (2011). Role of subchondral bone during early-stage experimental TMJ osteoarthritis. J Dent Res, 90(11), 1331–1338. doi: 10.1177/0022034511421930 [PubMed: 21917603]

Fan Y, Zhao L, Lai Y, Lu K, & Huang J (2022). CRISPR-Cas9-mediated loss of function of β-catenin attenuates intervertebral disc degeneration. Mol Ther Nucleic Acids, 28, 387–396. doi: 10.1016/j.omtn.2022.03.024 [PubMed: 35505959]

Glasson SS, Chambers MG, Van Den Berg WB, & Little CB (2010). The OARSI histopathology initiative - recommendations for histological assessments of osteoarthritis in the mouse. Osteoarthritis Cartilage, 18 Suppl 3, S17–23. doi: 10.1016/j.joca.2010.05.025 S1063–4584(10)00238–4 [pii]

Hill A, Duran J, & Purcell P (2014). Lubricin protects the temporomandibular joint surfaces from degeneration. PLoS One, 9(9), e106497. doi: 10.1371/journal.pone.0106497 PONE-D-14-19307 [pii] [PubMed: 25188282]

Huang J, Zhao L, & Chen D (2018). Growth factor signalling in osteoarthritis. Growth Factors, 36(5–6), 187–195. doi: 10.1080/08977194.2018.1548444 [PubMed: 30624091]

Huang J, Zhao L, Fan Y, Liao L, Ma PX, Xiao G, & Chen D (2019). The microRNAs miR-204 and miR-211 maintain joint homeostasis and protect against osteoarthritis progression. Nat Commun, 10(1), 2876. doi: 10.1038/s41467-019-10753-5 [PubMed: 31253842]

Huang J, Zhao L, Xing L, & Chen D (2010). MicroRNA-204 regulates Runx2 protein expression and mesenchymal progenitor cell differentiation. Stem Cells, 28(2), 357–364. doi: 10.1002/stem.288 [PubMed: 20039258]

Hui T, Zhou Y, Wang T, Li J, Zhang S, Liao L, … Chen D (2018). Activation of β-catenin signaling in aggrecan-expressing cells in temporomandibular joint causes osteoarthritis-like defects. Int J Oral Sci, 10(2), 13. doi: 10.1038/s41368-018-0016-z [PubMed: 29686224]

Kawaguchi H (2008). Endochondral ossification signals in cartilage degradation during osteoarthritis progression in experimental mouse models. Mol Cells, 25(1), 1–6. [PubMed: 18319608]

Koç N (2020). Evaluation of osteoarthritic changes in the temporomandibular joint and their correlations with age: A retrospective CBCT study. Dent Med Probl, 57(1), 67–72. doi: 10.17219/dmp/112392 [PubMed: 31997586]

Koyama E, Saunders C, Salhab I, Decker RS, Chen I, Um H, … Nah HD (2014). Lubricin is Required for the Structural Integrity and Post-natal Maintenance of TMJ. J Dent Res, 93(7), 663–670. doi: 0022034514535807 [pii] 10.1177/0022034514535807 [PubMed: 24834922]

Liao L, Zhang S, Zhou GQ, Ye L, Huang J, Zhao L, & Chen D (2019). Deletion of Runx2 in condylar chondrocytes disrupts TMJ tissue homeostasis. J Cell Physiol, 234(4), 3436–3444. doi: 10.1002/jcp.26761 [PubMed: 30387127]

Lu K, Ma F, Yi D, Yu H, Tong L, & Chen D (2022). Molecular signaling in temporomandibular joint osteoarthritis. J Orthop Translat, 32, 21–27. doi: 10.1016/j.jot.2021.07.001 [PubMed: 35591935]

Matheus HR, Özdemir Ş D, & Guastaldi FPS (2022). Stem cell-based therapies for temporomandibular joint osteoarthritis and regeneration of cartilage/osteochondral defects: a

systematic review of preclinical experiments. Osteoarthritis Cartilage, 30(9), 1174–1185. doi: 10.1016/j.joca.2022.05.006 [PubMed: 35597373]

Mori H, Izawa T, & Tanaka E (2015). Smad3 deficiency leads to mandibular condyle degradation via the sphingosine 1-phosphate (S1P)/S1P3 signaling axis. Am J Pathol, 185(10), 2742–2756. doi: 10.1016/j.ajpath.2015.06.015 S0002–9440(15)00385–5 [pii] [PubMed: 26272361]

Nah KS (2012). Condylar bony changes in patients with temporomandibular disorders: a CBCT study. Imaging Sci Dent, 42(4), 249–253. doi: 10.5624/isd.2012.42.4.249 [PubMed: 23301212]

Nickel JC, Iwasaki LR, Gonzalez YM, Gallo LM, & Yao H (2018). Mechanobehavior and Ontogenesis of the Temporomandibular Joint. J Dent Res, 97(11), 1185–1192. doi: 10.1177/0022034518786469 [PubMed: 30004817]

Schminke B, Muhammad H, Bode C, Sadowski B, Gerter R, Gersdorff N, … Miosge N (2014). A discoidin domain receptor 1 knock-out mouse as a novel model for osteoarthritis of the temporomandibular joint. Cell Mol Life Sci, 71(6), 1081–1096. doi: 10.1007/s00018-013-1436-8 [PubMed: 23912900]

Seidel MF, Wise BL, & Lane NE (2013). Nerve growth factor: an update on the science and therapy. Osteoarthritis Cartilage, 21(9), 1223–1228. doi: 10.1016/j.joca.2013.06.004 [PubMed: 23973134]

Shen J, Li J, Wang B, Jin H, Wang M, Zhang Y, … Chen D (2013). Deletion of the transforming growth factor beta receptor type II gene in articular chondrocytes leads to a progressive osteoarthritis-like phenotype in mice. Arthritis Rheum, 65(12), 3107–3119. doi: 10.1002/art.38122 [PubMed: 23982761]

Slade GD, Ohrbach R, Greenspan JD, Fillingim RB, Bair E, Sanders AE, … Maixner W (2016). Painful Temporomandibular Disorder: Decade of Discovery from OPPERA Studies. J Dent Res, 95(10), 1084–1092. doi: 10.1177/0022034516653743 [PubMed: 27339423]

Valesan LF, Da-Cas CD, Réus JC, Denardin ACS, Garanhani RR, Bonotto D, … de Souza BDM (2021). Prevalence of temporomandibular joint disorders: a systematic review and meta-analysis. Clin Oral Investig, 25(2), 441–453. doi: 10.1007/s00784-020-03710-w

van der Kraan PM, & van den Berg WB (2012). Chondrocyte hypertrophy and osteoarthritis: role in initiation and progression of cartilage degeneration? Osteoarthritis Cartilage, 20(3), 223–232. doi: 10.1016/j.joca.2011.12.003 [PubMed: 22178514]

Vidigal JA, & Ventura A (2015). The biological functions of miRNAs: lessons from in vivo studies. Trends Cell Biol, 25(3), 137–147. doi: 10.1016/j.tcb.2014.11.004 [PubMed: 25484347]

Wang M, Li S, Xie W, Shen J, Im HJ, Holz JD, … Chen D (2014). Activation of beta-catenin signalling leads to temporomandibular joint defects. Eur Cell Mater, 28, 223–235. doi: vol028a15 [pii] [PubMed: 25340802]

Wang XD, Zhang JN, Gan YH, & Zhou YH (2015). Current understanding of pathogenesis and treatment of TMJ osteoarthritis. J Dent Res, 94(5), 666–673. doi: 10.1177/0022034515574770 [PubMed: 25744069]

Zhang J, Jiao K, Zhang M, Zhou T, Liu XD, Yu SB, … Wang MQ (2013). Occlusal effects on longitudinal bone alterations of the temporomandibular joint. J Dent Res, 92(3), 253–259. doi: 10.1177/0022034512473482 [PubMed: 23340211]

Zhao L, Huang J, Fan Y, Li J, You T, He S, … Chen D (2019). Exploration of CRISPR/Cas9-based gene editing as therapy for osteoarthritis. Ann Rheum Dis, 78(5), 676–682. doi: 10.1136/annrheumdis-2018-214724 [PubMed: 30842121]

Zhao YP, Zhang ZY, Wu YT, Zhang WL, & Ma XC (2011). Investigation of the clinical and radiographic features of osteoarthrosis of the temporomandibular joints in adolescents and young adults. Oral Surg Oral Med Oral Pathol Oral Radiol Endod, 111(2), e27–34. doi: 10.1016/j.tripleo.2010.09.076

Zhou Y, Shu B, Xie R, Huang J, Zheng L, Zhou X, … Chen D (2019). Deletion of Axin1 in condylar chondrocytes leads to osteoarthritis-like phenotype in temporomandibular joint via activation of beta-catenin and FGF signaling. J Cell Physiol, 234(2), 1720–1729. doi: 10.1002/jcp.27043 [PubMed: 30070692]

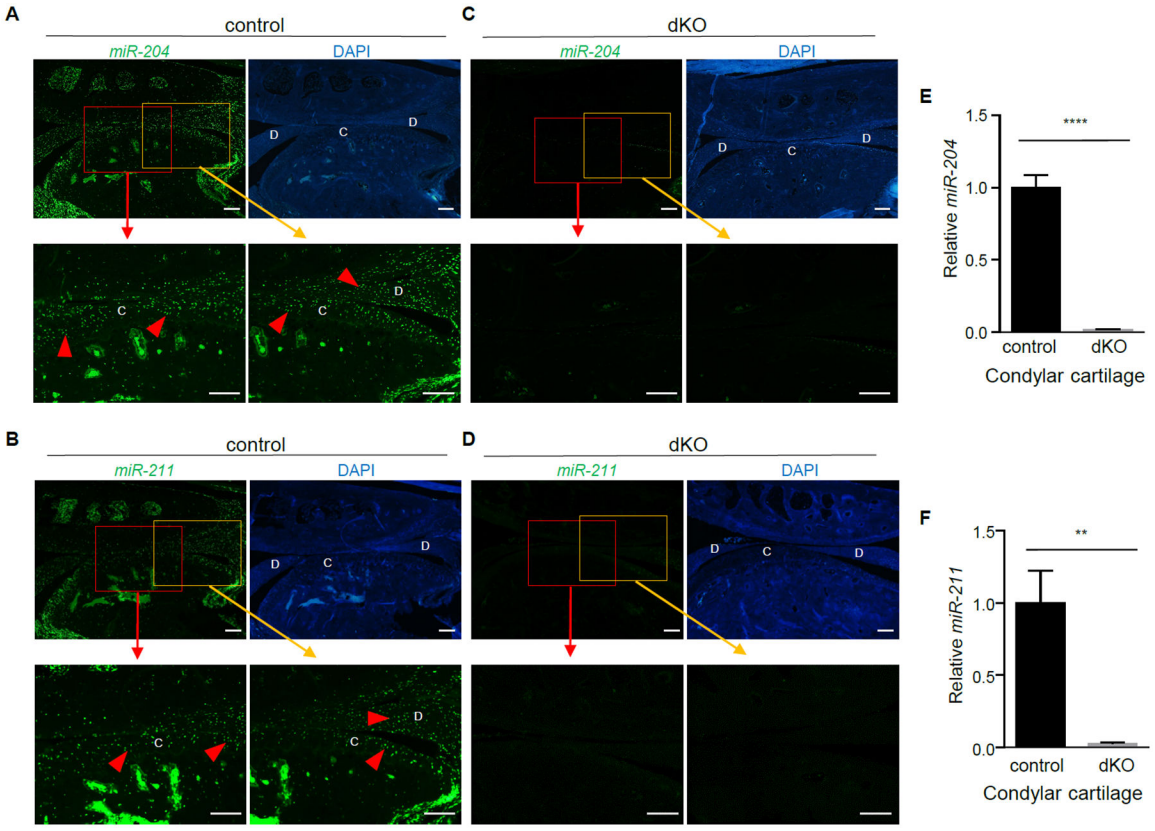

Figure 1.

Confirmation of the expression of *miR-204 and miR-211* in the TMJ and their deletions in the dKO mice. (**A, B**) In situ hybridization (ISH) using highly specific LNA-enhanced *miR-204* (**A**) or *miR-211* (**B**) probe (green) on TMJ sections of 8-month-old control (C57BL6/J) mice. The bottom panels are the enlargements of the upper images as indicated. DAPI staining marks nuclei (blue). Red arrowheads, *miR-204*- or *miR-211*-positive cells. (**C, D**) ISH of *miR-204* (**C**) or *miR-211* (**D**) in 8-month-old dKO TMJ. The bottom panels are the enlargements of the upper images as indicated. DAPI staining marks nuclei (blue). n = 5. Scale bars, 100 μm. C, condylar cartilage; D, articular disc. (**E, F**) quantitative PCR analysis of *miR-204* (**E**) and *miR-211* (**F**) in condylar cartilage from the control or dKO mice. ** $P < 0.01$, **** $P < 0.0001$, unpaired Student's *t*-test. n = 3. Data are shown as the mean ± s.d.

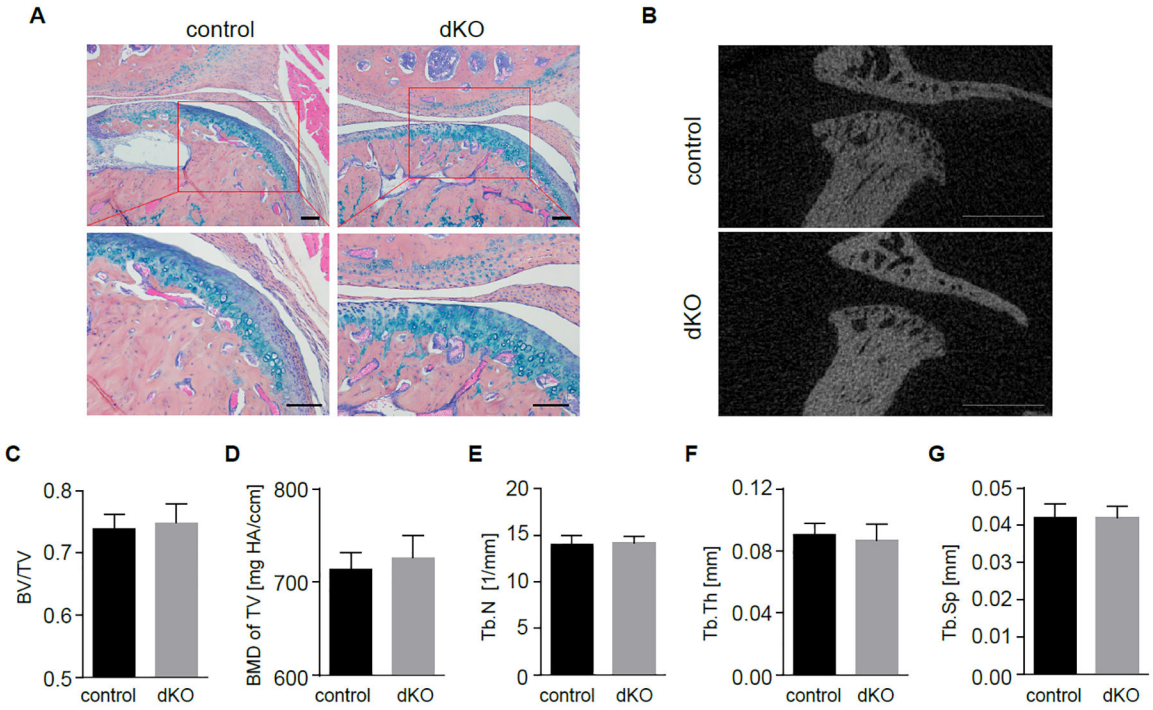

Figure 2.

The *miR-204/−211* double knockout mice show generally normal TMJ structure at a young age. (**A**) Representative histology images of the TMJs from 3-month-old *miR-204/−211* floxed (control) mice and constitutive double KO (dKO) mice stained by Alcian blue/ hematoxylin & orange G. Scale bars, 100 μm. (**B**) Representative μCT images of 3-month-old control and dKO mice. Scale bars, 1.0 mm. (**C-G**) Quantification of μCT results show normal bone properties of condylar subchondral bone in the dKO mice. n = 10. Unpaired Student's *t*-test. Data are shown as the mean ± s.d.

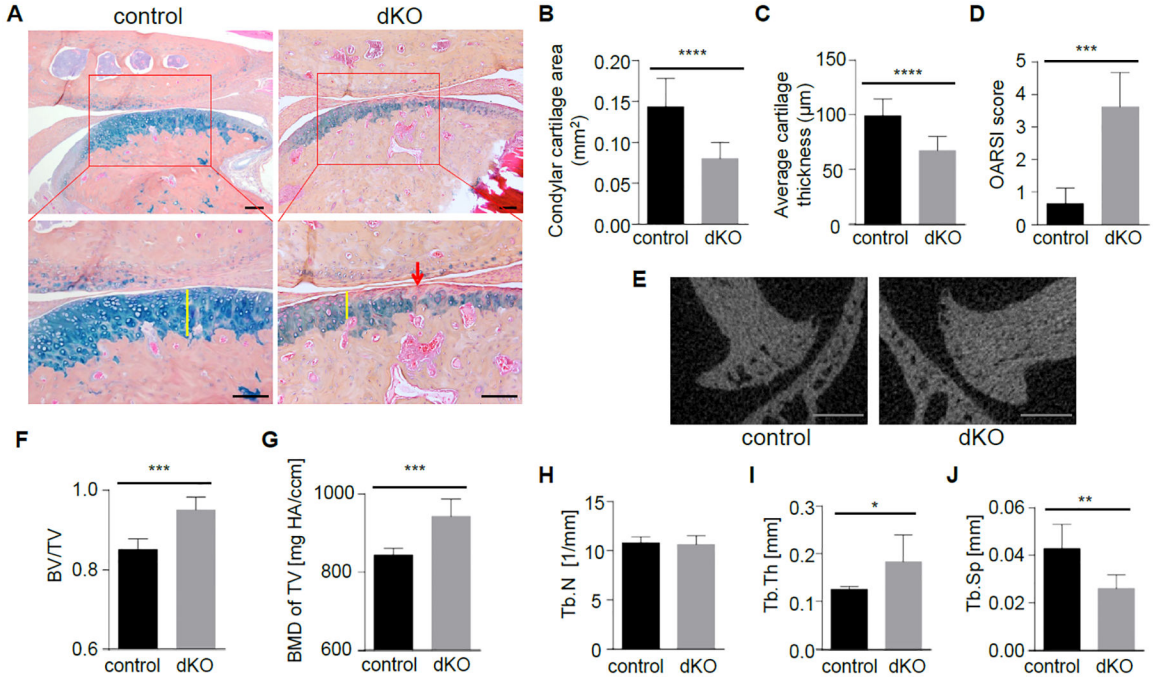

Figure 3.

Germline deletions of *miR-204/−211* cause TMJ OA in the aged mice. (**A**) Representative histology images of the TMJs of 8-month-old *miR-204/−211* floxed (control) mice and constitutive double KO (dKO) mice stained by Alcian blue/hematoxylin & orange G. Red arrow: proteoglycan loss; yellow bars: cartilage thickness. Scale bars, 100 μm. (**B, C**) Histomorphometric quantification of condylar cartilage area (**B**), and average cartilage thickness (**C**) of control and dKO mice. **** $P < 0.0001$, n = 7. (**D**) Osteoarthritis research society international (OARSI) scoring system was used to evaluate condylar cartilage destruction in 8-month-old control and dKO mice. *** $P < 0.001$, n = 7. (**E**) Representative μCT images of the TMJs in 8-month-old control and dKO mice. Scale bars, 500 μm. (**F-J**) μCT analysis shows abnormal remodeling of condylar subchondral bone in the dKO mice. * $P < 0.05$, ** $P < 0.01$, *** $P < 0.001$. n = 6. Unpaired Student's *t*-test. Data are shown as the mean ± s.d.

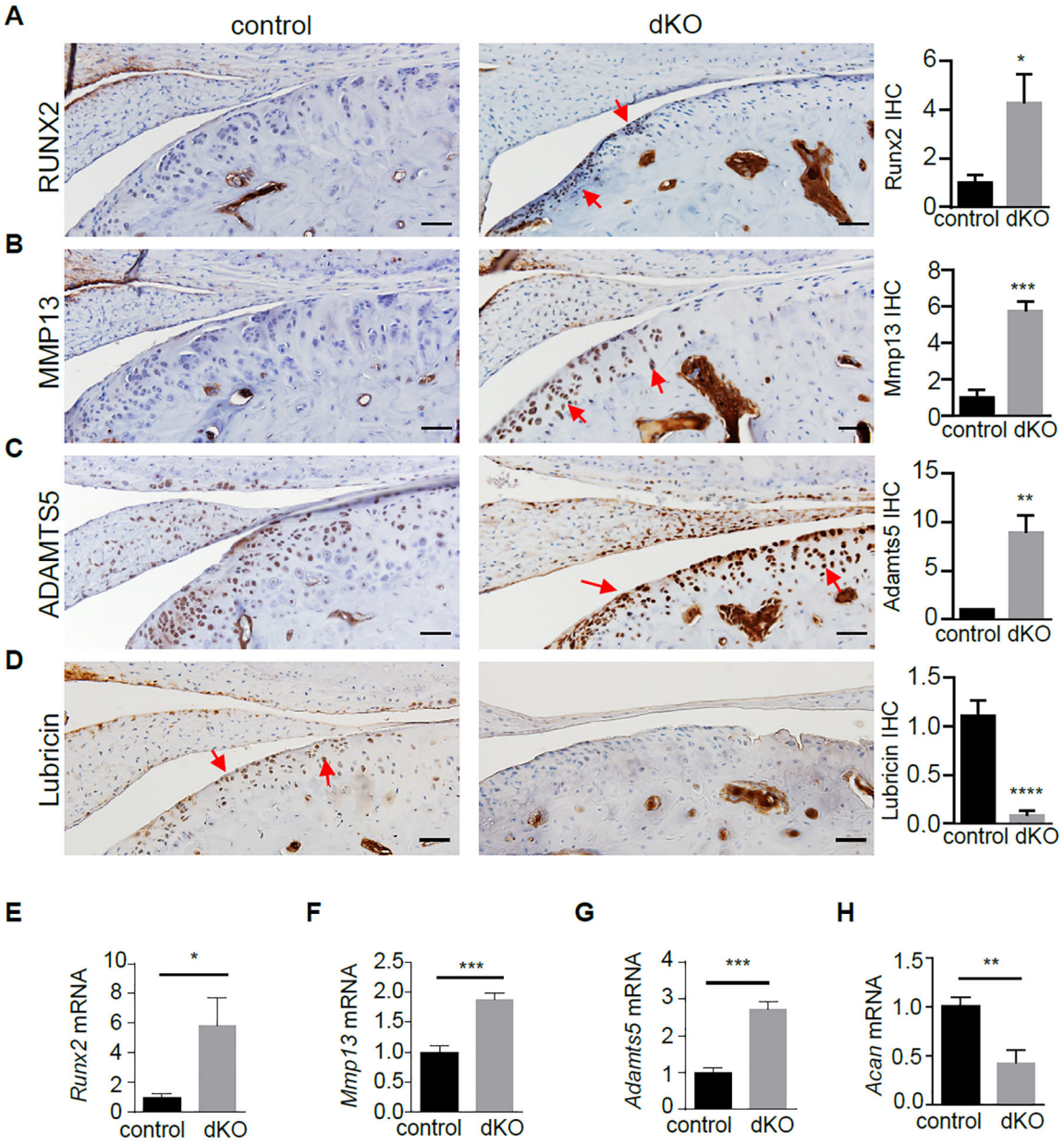

Figure 4.

The *miR-204/−211*-RUNX2 axis is essential for joint homeostasis. (**A-D**) Immunohistochemistry (IHC) results of RUNX2 (**A**), MMP13 (**B**), ADAMTS5 (**C**), and Lubricin (**D**) in the TMJs of the control and dKO mice. Red arrows, IHC-positive cells. Scale bars, 50 μm. Quantification of the IHC was performed by ImageJ. n = 3. (**E-H**) Quantitative RT-PCR analysis of *Runx2* (**E**), *Mmp13* (**F**), *Adamts5* (**G**), and *Aggrecan* (**H**) mRNAs in condylar cartilage from control or dKO mice. n = 3. * $P < 0.05$, ** $P < 0.01$, *** $P < 0.001$, **** $P < 0.0001$. Unpaired Student's *t*-test. Data are shown as the mean ± s.d.

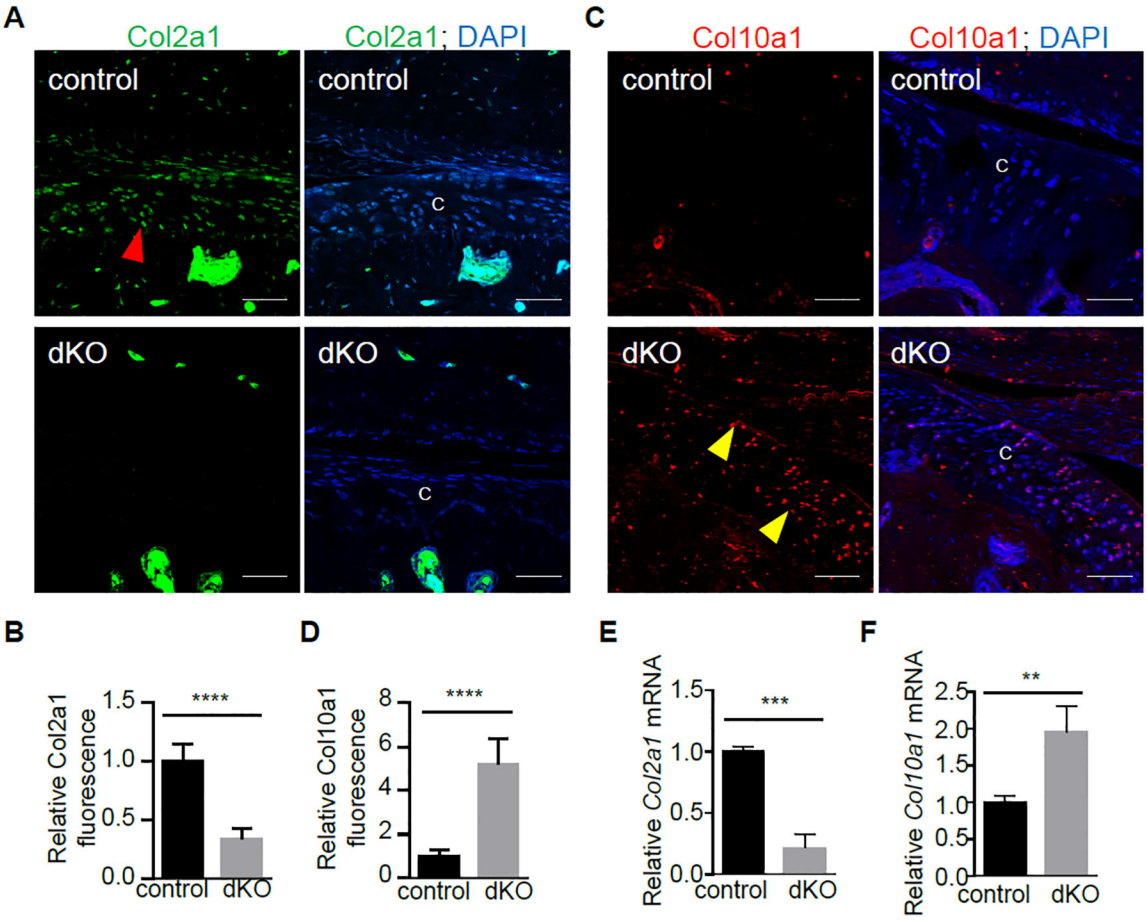

Figure 5.

Deficiency of *miR-204/−211* alters collagen composition in the TMJ. (**A**) IHC results of Col2a1 in the TMJs of control and dKO mice. Red arrowheads, Col2a1-positive cells. Scale bars, 25 μm. C, condylar cartilage. (**B**) Quantification of Col2a1-positive fluorescent intensity per area was performed by ImageJ. n = 6. (**C, D**) IHC results (**C**) and quantification (**D**) of Col10a1. Yellow arrowheads, Col10a1-positive cells. Scale bars, 25 μm. n = 6. C, condylar cartilage. (**E**) Quantitative RT-PCR analysis of *Col2a1* mRNAs in condylar cartilage from the control or dKO mice. n = 3. (**F**) Quantitative RT-PCR analysis of *Col10a1* mRNAs in condylar cartilage. n = 3. ** $P < 0.01$, *** $P < 0.001$, **** $P < 0.0001$. Unpaired Student's *t*-test. Data are shown as the mean ± s.d.

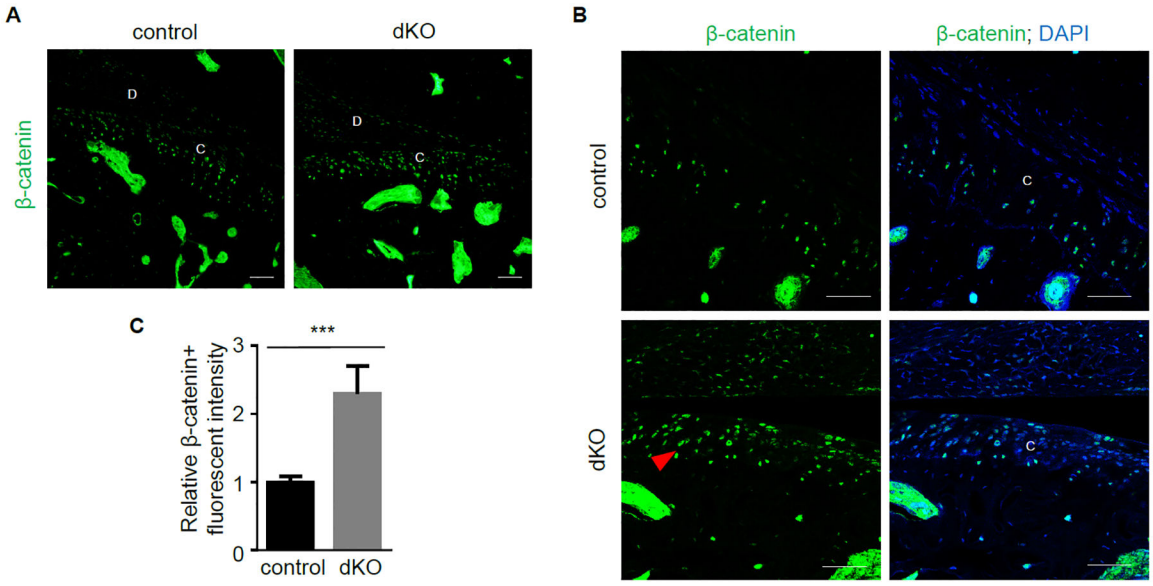

Figure 6.

Dysregulation of the β-catenin signaling by *miR-204/−211* loss-of-function. (**A, B**) Immunohistochemistry (IHC) of β-catenin in the control and dKO TMJ. Images of higher magnification (**B**) showed β-catenin expressions in the central region of condylar cartilage. Red arrowhead, β-catenin positive cells. C, condylar cartilage; D, articular disc. Scale bars, 50 μm (**A**) and Scale bars, 25 μm (**B**). (**C**) Quantification of positive β-catenin staining between the control and dKO condylar cartilage. n = 5. *** $P < 0.001$. Unpaired Student's *t*-test. Data are shown as the mean ± s.d.

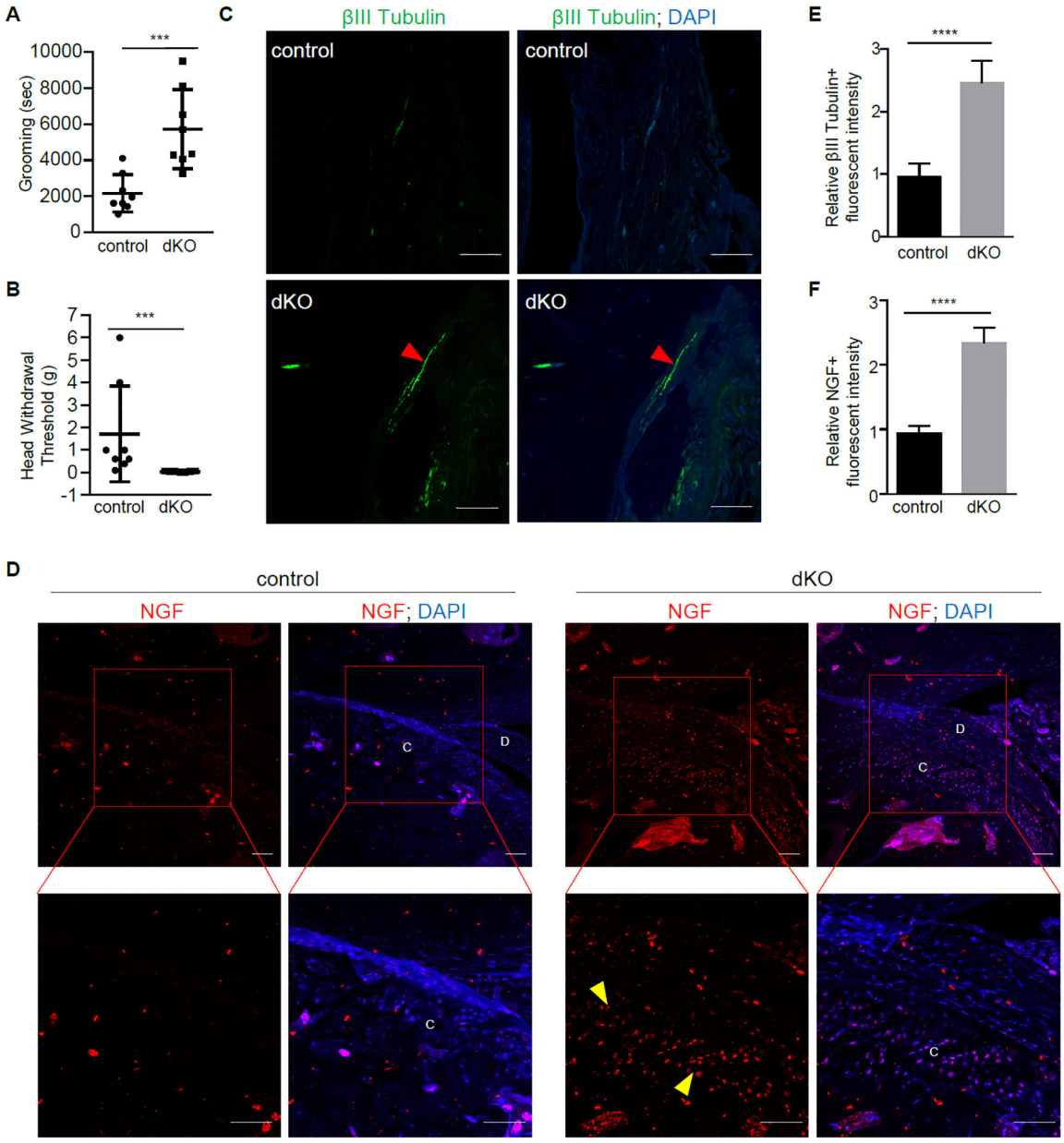

Figure 7.

Deficiency of *miR-204/−211* enhances TMJ OA pain. (**A**) Grooming behavior significantly increased in the dKO mice as assessed by the LABORAS system during 15-hr tests. n = 8. *** $P < 0.001$, unpaired Student's *t*-test. (**B**) Results of von Frey test of 8-month-old control and dKO mice. n = 8. *** $P < 0.001$, Mann-Whitney test. (**C, E**) Immunohistochemistry (IHC) results of βIII tubulin, a neuronal marker, was upregulated in the synovium of TMJ in dKO mice. Red arrowheads, βIII tubulin-positive cells. n = 6. Scale bars, 25 μm. (**D, F**) IHC results of NGF in the condylar cartilage. The bottom panels are the enlargements of the upper images as indicated. Yellow arrowheads, NGF-positive cells. C, condylar cartilage; D,

articular disc. n = 6. Scale bars, 25 μm. **** $P < 0.0001$, unpaired Student's *t*-test. Data are shown as the mean ± s.d.